Hydrothermal Synthesis of Sodium and Potassium Bismuth Titanates

Malgorzata M. Lencka,*,† Magdalena Oledzka,‡ and Richard E. Riman‡

OLI Systems, Inc., 108 American Road, Morris Plains, New Jersey 07950, and Department of Ceramic and Materials Engineering, Rutgers University, Piscataway, New Jersey 08854-8065

Received October 20, 1999. Revised Manuscript Received February 15, 2000

A thermodynamic model of electrolyte solutions has been used as a tool for equilibrium calculations in the Na−Bi−Ti−H_2O and K−Bi−Ti−H_2O systems. To perform the calculations, unknown standard-state properties for $Na_{0.5}Bi_{0.5}TiO_3$ (NBT), $K_{0.5}Bi_{0.5}TiO_3$ (KBT) and other solid compounds that exist in these systems were established. As a result of the calculations, stability and yield diagrams of the investigated systems were computed. Thus, the optimum conditions (i.e., temperature, synthesis precursor concentrations, solution pH) for the hydrothermal synthesis of phase-pure KBT and NBT are presented in a graphical form. They show the concentrations of precursors and pH-adjusting agents required for the formation of phase-pure alkaline bismuth titanates. The computed diagrams show that the formation of phase-pure sodium and potassium bismuth titanates takes place in highly alkaline solutions (e.g., at pH above 11.4 and 12.2, respectively, at 473 K). Results of our experiments validated the newly developed yield diagrams and demonstrated, for the first time, that alkaline bismuth titanates can be hydrothermally synthesized. Experimental synthesis was carried out using both conventional and microwave-heated reactors.

Introduction

The increasing demand for environmentally benign materials and manufacturing processes points in the direction of lead-free ceramic materials for electronic applications. Materials of great importance include perovskite-type compounds such as alkali metal bismuth titanates and niobates represented by $(Na,K)_{0.5}Bi_{0.5}TiO_3$ and $(Na,K)NbO_3$, bismuth-layer-structured compounds such as $Bi_4Ti_3O_{12}$ or $SrBi_2Nb_2O_9$, and tungsten-bronzes (e.g., $(Sr,Ba)Nb_2O_6$).[1] Ferroelectric and piezoelectric properties of potassium bismuth titanate $K_{0.5}Bi_{0.5}TiO_3$ (KBT) and sodium bismuth titanate $Na_{0.5}Bi_{0.5}TiO_3$ (NBT) were studied and reported in the early 1960s by Smolenski et al.[2] and Jaffe et al.[3] Both KBT and NBT are strongly ferroelectric materials with relatively high Curie temperatures of 653 and 593 K, respectively.[2] Also, pyroelectric properties of NBT and KBT were reported[4,5] and a positive temperature coefficient of resistivity (PTCR) effect was observed in alkaline bismuth titanates. This effect was thoroughly investigated by several authors[4,6−7]

It is well-known that solid solutions with compositions close to a morphotropic phase boundary exhibit promising electromechanical properties. Dielectric and piezoelectric properties of KBT-NBT solid solutions were investigated by many authors.[7−11] Hong[10] and Elekechai[11] found the range of compositions where the NBT-KBT solid solutions show the most pronounced piezoelectric characteristics for materials without lead. It was also demonstrated that solid solutions between NBT or/and KBT and other solid compounds (i.e., perovskites or bismuth-layer-structured or tungsten-bronze-type materials) possess promising piezoelectric and pyroelectric properties which are associated with the presence of morphotropic regions.[12−15]

Potassium bismuth titanate exhibits a tetragonal symmetry while sodium bismuth titanate has a rhombohedral crystallographic structure. Unit cell parameters of potassium and sodium bismuth titanates were reported by many authors.[2−3,11,16−18] In general, lattice parameters measured by various investigators are in close agreement. It should be noted that both lattice

* Corresponding author. E-mail: mlencka@olisystems.com.
† OLI Systems, Inc.
‡ Rutgers University.

(1) Swartz, S. L.; Shrout, T. R.; Takenaka, T. *Am. Ceram. Soc. Bull.* **1997**, *76*, 51.
(2) Smolenski, G. A.; Isupov, V. A.; Agranovskaya, A. I.; Krainik, N. N. *Soviet Physics-Solid State* **1961**, *2*, 2651.
(3) Jaffe, B.; Cook, W. R., Jr.; Jaffe, H. Piezoelectric Ceramics. In *Non-Metallic Solids. A Series of Monographs*; Roberts, J. P., Popper, P., Eds.; Academic Press: New York, 1971; Vol. 3.
(4) Fu, B.; Chen, Z.; Bai, T.; Liu, M. *Ferroelectrics* **1990**, *101*, 219.
(5) Gadzev, M. S.; Ismailizade, I. G.; Abiev, A. K. *Ferroelectrics* **1984**, *4*, 1502.
(6) Vakhrushev, S. B.; Isupov, V. A.; Kvyatkovsky, B. E.; Okuneva, N. M.; Pronin, I. P.; Smolensky, G. A.; Syrnikov, P. P. *Ferroelectrics* **1985**, *63*, 153.
(7) Raevski, I. P.; Emelyanov, S. M.; Bokov, A. A.; Popov, Yu. M.; Pavlov, A. N. *J. Technol. Phys.* **1988**, *58*, 1746.
(8) Pronin, I. P.; Parfenova, N. N.; Zaitzev, N. B.; Isupov, V. A.; Smolenskii, G. A. *Fiz. Tverd. Tela* **1982**, *24*, 1860.
(9) Wang, T.; Wang, L.; Lu, Y.; Zhou, D. *Guisuanyan Xuebao* **1987**, *15*, 248.
(10) Hong, W. *Sci. Ceram.* **1984**, *12*, 709.
(11) Elekechai, O.; Manier, M.; Mercurio, J. P. *Phys. Stat. Sol.(a)* **1996**, *157*, 499.
(12) Takenaka, T.; Sakata, K.; Toda, K. *Ferroelectrics* **1990**, *106*, 375.
(13) Takenaka, T.; Sakata, K. *Ferroelectrics* **1989**, *94*, 175.
(14) Antonenko, A. M.; Gavshin, M. G.; Kudzin, A. Yu. *Phys. Solid. State* **1997**, *39*, 1281.
(15) Elkechai, O.; Marchet, P.; Thomas, P.; Manier, M.; Mercurio, J.-P. *J. Mater. Chem.* **1997**, *7*, 91.

10.1021/cm9906654 CCC: $19.00
Published on Web 04/07/2000

parameters and electrical properties for KBT and NBT were reported for solid compounds prepared by a conventional ceramic sintering of bismuth and titanium oxides with sodium and potassium carbonates at high temperatures (i.e., 1123−1423 K). Equilibria in the Bi_2O_3−TiO_2−NaOH hydrothermal system at supercritical conditions (i.e., at temperature of 723 K and pressure of 400−1000 atm) were studied by Kurazhkovskaya.[19] Experiments were performed at NaOH concentrations varying from 0 to 10 M (10.8 m) and at constant concentration of water (i.e., 60−70 wt %). $Na_{0.5}Bi_{0.5}TiO_3$ was one of seven crystalline phases that formed in the above system.

Hydrothermal synthesis of ceramic powders has gained considerable popularity because it has the potential to yield high-purity, homogeneous, fine crystalline powders at moderate conditions.[20,21] Hydrothermal synthesis does not require expensive precursors and elaborate apparatus. Moreover, it is possible to predict the optimum synthesis conditions using theoretical methods based on electrolyte thermodynamics.[22,23] Optimal synthesis conditions are shown in a very convenient form with phase stability and yield diagrams.[24] In this work, we focus on the hydrothermal synthesis of phase-pure potassium and sodium bismuth titanates. For this purpose, both thermodynamic modeling and experiment validation are important. We further verify our predictions by performing the synthesis at optimum conditions using both conventional and microwave hydrothermal techniques.

Thermodynamic Modeling

The thermodynamic model is used to predict equilibria in multicomponent systems that may contain an aqueous phase, any number of solid phases and, if necessary, a vapor and a nonaqueous liquid phase. As a result of the computation of chemical and phase equilibria, we obtain concentrations and activity coefficients of all aqueous species and amounts of precipitated solid phases. For this purpose, a realistic model of electrolyte systems is used. This model combines information about standard-state properties of all species of interest with a formulation for the excess Gibbs energy, which accounts for solution nonideality. The model has been described in detail by Zemaitis et al.[25] and Rafal et al.[26] This model is a part of the OLI software.[27] It has been successfully applied to the hydrothermal synthesis of various perovskite-type materials.[22−24,28−29] Also, the model has been extensively validated experimentaly.[23−24,28−29]

1. Standard-State Properties for New Solids. It has been previously shown[22] that the key parameters for calculating the speciation in the system of interest are standard-state properties of all aqueous (both ionic and neutral) species that exist in the solution and all solid species that may precipitate from the solution. The standard-state properties include the standard Gibbs energy $\Delta_f G°$ and enthalpy $\Delta_f H°$ of formation, and absolute entropy $S°$ at a reference temperature (usually 298.15 K) as well as partial molar volume V^o and heat capacity C_p^o as functions of temperature. The OLI data bank[27] contains this information for many aqueous, gaseous, and solid species. They were taken from critically evaluated and consistent sources.[22] It should be noted, however, that in the case of solid compounds, solubility data in water as well as in alkaline and/or acidic solutions at different temperatures are the best source of standard-state properties. The solubility data are available in the book of Seidell[30] and Linke[31] and in the current literature. Whenever possible, regression of solubility data has been performed using the OLI software to obtain accurate and consistent thermochemical data for solid compounds. Various predictive methods based on a family analysis or group contribution methods are also considered[32−34] when no experimental data are available.

In practical applications, we are frequently dealing with systems in which various complex solid phases may precipitate. Such phases may not have been investigated before and, therefore, their thermochemical properties are unknown. In these cases, it is advantageous to run calculations and experiments simultaneously. Experiments may contribute somewhat to the correction of the existing or estimated thermochemical properties. They may also supply new information regarding solids that exist in real hydrothermal systems but were not considered in our calculations.

The chemical identity of chemical species in a system of interest depends on the selected set of precursors. In our work, equilibrium calculations are performed for the hydrothermal system obtained by mixing bismuth nitrate pentahydrate, titanium oxide, and sodium or potassium hydroxide in water. In this case, the thermodynamic model is formulated for 26 independent reactions involving 32 aqueous, gaseous and solid species. Table 1 shows species that are considered in modeling the K−Bi−Ti−H_2O system. It should be noted that the standard-state properties for all 32 species are necessary for the thermodynamic computations in this system. Data for most species from Table 1 were published in our previous studies.[22−23,28] For aqueous

(16) Buhrer, C. F. *J. Chem. Phys.* **1962**, *36*, 798.
(17) Guo, Ch.; Wu, Y.; Wang, T. *Wuli Xuebao (Acta Phys. Sinica)* **1982**, *31*, 1119.
(18) Ivanova, V. V.; Kapyshev, A. G.; Venevtsev, Yu. N.; Zhdanov, G. S. *Izv. Akad. Nauk SSSR, Ser. Fiz.* **1962**, *26*, 354.
(19) Kurazhkovskaya, V. S. *Vest. Mosk. Univ., Geol.* **1976**, *31*, 109.
(20) Dawson, W. J. *Ceram. Bull.* **1988**, *67*, 1673.
(21) Segal, D. *J. Mater. Chem.* **1997**, *7*, 1297.
(22) Lencka M. M.; Riman, R. E. *Chem. Mater.* **1993**, *5*, 61.
(23) Lencka, M. M.; Riman, R. E. *J. Am. Ceram. Soc.* **1993**, *76*, 2649.
(24) Lencka, M. M.; Nielsen, E.; Anderko, A.; Riman, R. E. *Chem. Mater.* **1997**, *9*, 1116.
(25) Zemaitis, J. F., Jr.; Clark, D. M.; Rafal, M.; Scrivner, N. C. *Handbook of Aqueous Electrolyte Thermodynamics: Theory & Application*; American Institute of Chemical Engineers, Inc.: New York, 1986.
(26) Rafal, M.; Berthold, J. W.; Scrivner, N. C.; Grise, S. L. *Models for Thermodynamic and Phase Equilibria Calculations*; Sandler, S. I., Ed.; Marcel Dekker: New York, 1994; p 601.
(27) OLI Software, Environmental and Corrosion Simulation Programs (ESP/CSP), OLI Systems, Inc., Morris Plains, NJ, 1996.
(28) Lencka, M. M.; Riman, R. E. *Chem. Mater.* **1995**, *7*, 18.
(29) Lencka, M. M.; Anderko, A.; Riman, R. E. *J. Am. Ceram. Soc.* **1995**, *78*, 2609.
(30) Seidell, A. *Solubilities of Inorganic and Metal-Organic Compounds*, 4th ed.; American Chemical Society: Washington, DC, 1958; Vol. 1.
(31) Linke, W. F.; Seidell, A. *Solubilities of Inorganic and Metal-Organic Compounds*, 4th ed.; American Chemical Society: Washington, DC, 1965; Vol. 2.
(32) Latimer, W. *The Oxidation State of Elements and Their Potentials in Aqueous Solutions*, 2nd ed.; Prentice Hall: New York, 1952.
(33) Lencka, M. M.; Riman, R. E. *Thermochim. Acta* **1995**, *256*, 193.
(34) Kubaschewski, O.; Ünal, H. *High Temp.-High Pres.* **1977**, *9*, 361.

Table 1. Solid, Aqueous and Gaseous Species in the K−Bi−Ti−H_2O System

solid species	aqueous species	gaseous species
$K_{0.5}Bi_{0.5}TiO_3$	Bi^{3+}	H_2O
$Bi_4Ti_3O_{12}$	$BiOH^{2+}$	HNO_3
$Bi(NO_3)_3{\cdot}5H_2O$	$Bi(OH)_2^+$	
Bi_2O_3	$Bi(OH)_3$	
TiO_2(rutile)	$Bi(OH)_4^-$	
TiO_2(anatase)	$BiNO_3^{2+}$	
K_2TiO_3	$Bi(NO_3)_2^+$	
KOH	Ti^{4+}	
$KOH{\cdot}H_2O$	$TiOH^{3+}$	
$KOH{\cdot}2H_2O$	$Ti(OH)_2^{2+}$	
KNO_3	$Ti(OH)_3^+$	
	$Ti(OH)_4$	
	$HTiO_3^-$	
	K^+	
	NO_3^-	
	HNO_3	
	H^+	
	OH^-	
	H_2O	

bismuth species, thermochemical data of Shock et al.[35] were used. Here, we concentrate on solid compounds in the K−Bi−Ti−H_2O and Na−Bi−Ti−H_2O systems for which thermochemical properties have been calculated in this work from solubility data or were estimated. In particular, new thermochemical data have been established for Bi_2O_3, $Bi(NO_3)_3{\cdot}5H_2O$, $Bi_4Ti_3O_{12}$, K_2TiO_3, Na_2TiO_3, $K_{0.5}Bi_{0.5}TiO_3$, and $Na_{0.5}Bi_{0.5}TiO_3$. We do not consider other bismuth titanates except for $Bi_4Ti_3O_{12}$. However, we are aware of the fact that this solid phase is not the only stable phase in the Bi−Ti−H_2O system at various ratios of Bi and Ti in the precursor system. This will be reported in a future paper on the hydrothermal synthesis of bismuth titanate.[36]

Calculations of the solubility of bismuth oxide based on standard-state properties reported in the literature[37] did not agree with results of our experiments. Experiments showed that Bi_2O_3 was much less stable in the hydrothermal environment than other solid phases such as bismuth titanate ($Bi_4Ti_3O_{12}$) or alkaline bismuth titanates (KBT or NBT). Therefore, an attempt was done to recalculate its properties. The solubility of bismuth oxide in the binary NaOH−H_2O system of various concentrations at room temperature can be found in the book of Seidell.[31] These data were used to calculate the Gibbs energy of formation of Bi_2O_3. Absolute entropy and heat capacity as a function of temperature were taken from the compilation of Robie and Hemingway.[38] Subsequently, the enthalpy of formation was calculated using standard thermodynamic relationships.

Thermodynamic properties for bismuth nitrate pentahydrate were not available in the literature. However, the solubility of this hydrate in the binary HNO_3−H_2O system at room temperature was measured.[31] These data allowed us to calculate the Gibbs energy of formation of $Bi(NO_3)_3{\cdot}5H_2O$. Entropy and heat capacity were calculated using group contribution methods.[32,34]

Thermochemical properties of Na_2TiO_3 are available in the compilation of Barin.[39] Therefore, these data were first used in our calculations. However, computational results showed that sodium titanate precipitates at high pH and is much more stable than sodium bismuth titanate. This did not agree with experimental results where Na_2TiO_3 has never been observed. Thus, the thermochemical data were revised and calculated as a sum of the standard-state properties for the corresponding oxides (i.e., Na_2O and TiO_2). This procedure is commonly used as a first approximation in our calculations. The calculations based on the revised data showed that sodium titanate was not stable in water and alkaline solutions, which was in close agreement with our experimental results. The same computational approach was applied to K_2TiO_3 and $Bi_4Ti_3O_{12}$ for which data were not available in the literature. In the case of bismuth titanate, the standard-state properties were calculated from contributions of Bi_2O_3 and TiO_2.

In the first approximation, Gibbs energies of formation of $K_{0.5}Bi_{0.5}TiO_3$ and $Na_{0.5}Bi_{0.5}TiO_3$ were calculated as a sum of corresponding $\Delta_fG°$ for constituent oxides (i.e., TiO_2, K_2O, or Na_2O and Bi_2O_3). After unknown standard-state properties for other solids were calculated, the first approximations of $\Delta_fG°$ for NBT and KBT were slightly corrected. Reproducible experimental data served as a guide in the process for data refinement. Absolute entropies and heat capacities were calculated from entropies of constituent oxides. Then, enthalpies of formation were computed using standard thermodynamic relationships. Table 2 contains the standard-state properties that were developed in this work.

2. Stability and Yield Diagrams. As a result of repetitive application of our thermodynamic model for different input concentrations of sodium or potassium, bismuth and titanium precursors as well as pH-adjusting agents (mineralizers), we obtain a sufficient number of equilibrium points to construct stability and yield diagrams of the investigated systems. In general, stability diagrams show stability areas of aqueous and solid species in the system at equilibrium. At the same time, yield diagrams show the optimum synthesis conditions for the formation of a phase-pure solid compound of interest. Stability and yield diagrams are shown as a function of selected variables such as input metal concentrations on the *y* axis and solution pH on the *x* axis. However, different variables are also possible (i.e., temperature or pH-adjusting agent concentration). The interpretation of stability and yield diagrams was described in detail in our previous papers.[23−24,28−29] Here, we describe stability and yield diagrams in the K−Bi−Ti and Na−Bi−Ti hydrothermal systems at 473 K. These systems were obtained by mixing $Bi(NO_3)_3{\cdot}5H_2O$ and TiO_2 in the proportions corresponding to their stoichiometry in NBT or KBT with various amounts of NaOH or KOH. Alkaline hydroxides served as A-site metal suppliers to the perovskite structure as well as pH-adjusting agents in the reactions of formation of KBT and NBT.

(35) Shock, E. L.; Sassani, D. C.; Willis, M.; Sverjensky, D. A. *Geochim. Cosmochim. Acta* **1997**, *61*, 907.

(36) Lencka, M. M.; Hencken, R.; Riman, R. E. Manuscript in preparation.

(37) Gluschko, V. P. Ed. *Thermal Constants of Substances*; VINITI, Moscow, 1968; Vol. 3.

(38) Robie, R. A.; Hemingway, B. S.; Fisher, J. R. *Thermodynamic Properties of Minerals and Related Substances at 298.15 K and 1 Bar (10^5 Pascals) Pressure and at Higher Temperatures*; U. S. Geological Survey Bulletin 1452; U.S. Government Printing Office: Washington, DC, 1979.

(39) Barin, I., in collaboration with Sauert, F.; Schultze-Rhonhof, E.; Shu Sheng, W., *Thermochemical Data of Pure Substances*; VCH Publishers: New York, 1989 and 1993.

Table 2. Standard-State Properties of Solid Species in the Na−Bi−Ti and K−Bi−Ti Hydrothermal Systems

solid species	Bi_2O_3	$Bi(NO_3)_3{\cdot}5H_2O$	Na_2TiO_3	K_2TiO_3	$Bi_4Ti_3O_{12}$	$Na_{0.5}Bi_{0.5}TiO_3$	$K_{0.5}Bi_{0.5}TiO_3$
$\Delta G_f°$ (J·mol^{-1})	−489 668	−1 439 241	−1 259 060	−1 204 460	−3 644 070	−1 156 000	−1 163 500
$\Delta H_f°$ (J·mol^{-1})	−570 043	−2 030 202	−1 353 290	−1 300 420	−3 972 180	−1 241 578	−1 249 924
$S°$(J·mol^{-1}·K^{-1})	151.500	450.348	124.947	145.909	449.341	105.280	109.133
$C_p°$ (J·mol^{-1}·K^{-1})[a]	113.550	419.300	124.391	127.270	392.613	100.901	101.621
a (J·mol^{-1}·K^{-1})	103.602	419.300	136.077	120.956	403.268	110.640	106.860
$b \times 10^3$ (J·mol^{-1}·K^{-1})	33.356	0	34.639	78.779	118.263	26.644	37.679
$c \times 10^{-5}$ (J·mol^{-1}·K)	0	0	−19.601	−15.298	−40.912	−15.751	−14.675
$V° \times 10^6$ (m^3·mol^{-1})	49.730	97.014			145.72	70.656	74.184
references	this work, 30, 38	this work, 30, 32, 34	this work	this work	this work, 40	this work, 40	this work, 40

[a] Heat capacities are calculated from the relation $C_p° = a + bT + cT^{-2}$.

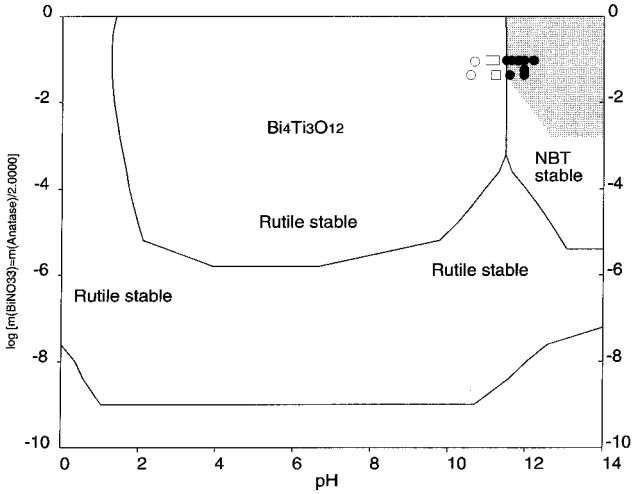

Figure 1. Calculated stability and yield diagram in the Na−Bi−Ti−H_2O system at 473 K as a function of solution pH. The symbols denote experimental conditions for which the following products were obtained: ○, $Bi_4Ti_3O_{12}$ + TiO_2; □, $Bi_4Ti_3O_{12}$ + TiO_2 + $Na_{0.5}Bi_{0.5}TiO_3$; and ●, $Na_{0.5}Bi_{0.5}TiO_3$.

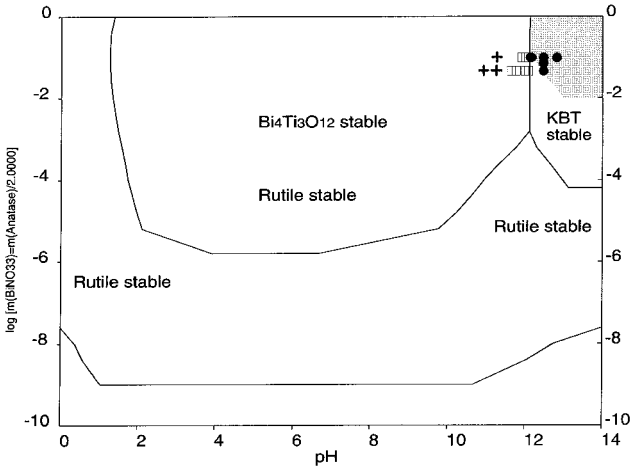

Figure 2. Calculated stability and yield diagram in the K−Bi−Ti−H_2O system at 473 K as a function of solution pH. The symbols denote experimental conditions for which the following products were obtained: +, $Bi_4Ti_3O_{12}$ + TiO_2 + an unknown phase; □, $Bi_4Ti_3O_{12}$ + TiO_2 + $K_{0.5}Bi_{0.5}TiO_3$; and ●, $K_{0.5}Bi_{0.5}TiO_3$.

Figures 1 and 2 show stability regions of various solid materials (i.e., $Bi_4Ti_3O_{12}$, TiO_2, KBT, and NBT) and yields of NBT and KBT in the investigated systems. Stability areas of $Bi_4Ti_3O_{12}$, TiO_2 (rutile), and KBT or NBT, which are denoted by solid lines, partly overlap with each other. In particular, rutile is stable practically in the whole pH range and in a wide concentration range of the input concentration of bismuth precursor

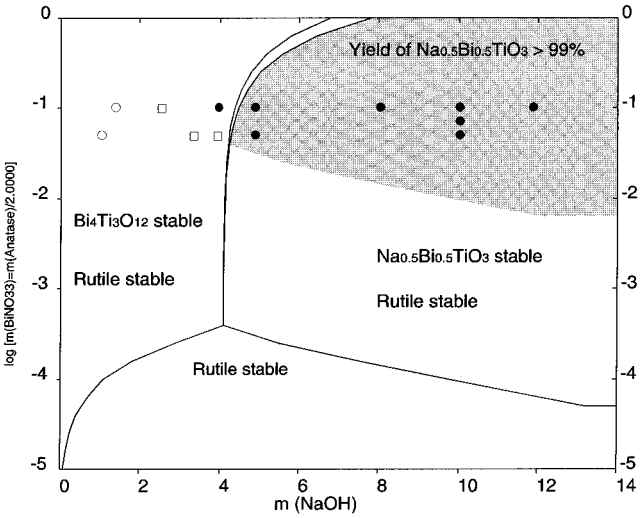

Figure 3. Calculated stability and yield diagram in the Na−Bi−Ti−H_2O system at 473 K as a function of NaOH concentration. The symbols denote experimental conditions for which the following products were obtained: ○, $Bi_4Ti_3O_{12}$ + TiO_2; □, $Bi_4Ti_3O_{12}$ + TiO_2 + $Na_{0.5}Bi_{0.5}TiO_3$; and ●, $Na_{0.5}Bi_{0.5}TiO_3$.

(i.e., above 10^{-9} m). The line that encompasses the pH region between slightly more than 1 and 11.4 (cf. Figure 1) or 12.0 (cf. Figure 2), and the input concentration of bismuth precursor between 10^{-6} and 1 m denotes the beginning of precipitation of bismuth titanate. Both $Bi_4Ti_3O_{12}$ and TiO_2 are stable in this area. A parabolic character of this line reflects the amphoteric character of bismuth. Solid lines located in the upper right corner of Figures 1 and 2 denote the beginning of precipitation of NBT and KBT, respectively. Sodium or potassium bismuth titanate and rutile are stable within these regions. In particular, KBT precipitates at pH above 12 and at the bismuth nitrate concentration above about 10^{-4} m. NBT starts to form in slightly less alkaline solutions and at lower precursor concentrations (i.e., for pH above 11.4 and bismuth concentration above about 10^{-5} m).

Also, the conditions for the synthesis of phase-pure NBT and KBT are shown in Figures 1 and 2 as shaded areas. They lie within the stability regions of sodium and potassium bismuth titanates and cover a relatively small interval of the synthesis conditions. Thus, the synthesis of phase-pure sodium and potassium bismuth titanates takes place at highly alkaline solutions. To visualize this, yield diagrams are constructed with the amounts of NaOH (cf. Figure 3) and KOH (cf. Figure 4) on the x axis while the y axis remains the same. It is very convenient to use this type of plot for experimental synthesis because it depicts the exact concentrations of precursors as well as mineralizers for the formation of

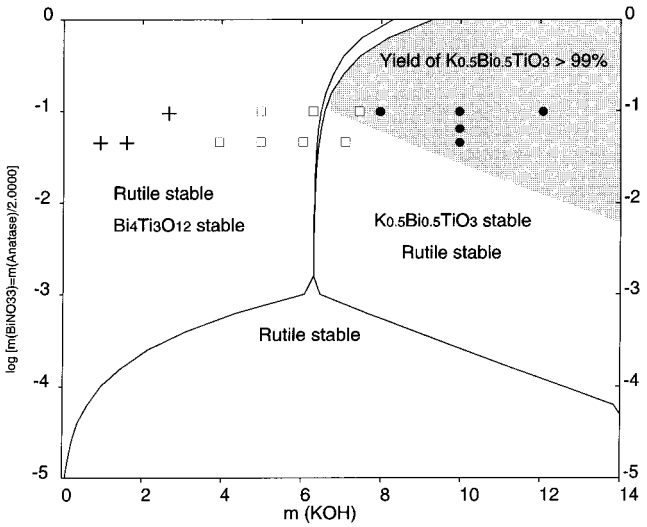

Figure 4. Calculated stability and yield diagram in the K−Bi−Ti−H_2O system at 473 K as a function of KOH concentration. The symbols denote experimental conditions for which the following products were obtained: +, $Bi_4Ti_3O_{12}$ + TiO_2 + an unknown phase; □, $Bi_4Ti_3O_{12}$ + TiO_2 + $K_{0.5}Bi_{0.5}TiO_3$; and ●, $K_{0.5}Bi_{0.5}TiO_3$.

phase-pure materials. Thus, pure KBT will form at the concentration of KOH above about 6 m and at relatively high concentrations of bismuth nitrate (above 0.01 m). At the similar bismuth precursor concentrations, NBT precipitates at the NaOH concentration as low as 4 m. In practice, Figures 3 and 4 served to define the optimum synthesis conditions for the preparation of pure NBT and KBT materials. In particular, the conditions within the shaded areas were used to synthesize phase-pure NBT and KBT. Also, selected conditions were verified experimentally in order to evaluate the calculated stability and yield diagrams.

Experimental Section

1. Reagents. Bismuth nitrate pentahydrate $Bi(NO_3)_3 \cdot 5H_2O$ (Johnson Matthey, Alfa Aesar, Ward Hill, MA, >97 wt % on metal basis), titanium dioxide TiO_2 (P25, Degussa, Dublin, OH), KOH (Fisher Scientific, Fair Lawn, NJ, about 12.5 wt % of water) and NaOH (Alfa Aesar, >97 wt % pure) were used as precursors in the hydrothermal synthesis of sodium and potassium bismuth titanates. At the same time, alkaline hydroxides were used to adjust the required solution pH values according to Figures 1−4. A stoichiometric ratio of titanium to bismuth (i.e., Ti/Bi = 2) in starting materials was employed in the reactions. Reactions with the input concentration of bismuth nitrate equal to 0.05 and 0.1 m were investigated.

2. Hydrothermal Synthesis. The synthesis of phase-pure NBT and KBT powders was performed using a conventional hydrothermal method and a microwave−hydrothermal technique. Reactions were carried out at 473 K and autogenous pressure either with or without stirring. The reaction time was set to 72 h to ensure complete equilibration. The influence of shorter reaction time (as short as 8 h) and lower temperature (i.e., 453 K) on the phase purity was also investigated. For this purpose, reactions in the phase-pure region were carried out with the input concentration of bismuth nitrate and alkaline hydroxide equal to 0.1 and 10 m, respectively.

In a conventional hydrothermal method, the reagents were charged into 110 mL stainless steel Teflon-lined autoclaves (Acid Digestion Bomb: Parr Instrument Company, Moline, IL) along with 50 g of double distilled deionized water. The autoclaves were placed into a box-type oven (Fisher) with a temperature control of ±1 K for the reactions without stirring. Reaction vessels where stirring was employed were heated by a close-fitting insulating mantle (Glas-Col, Terre Haute, IN) placed on a hot plate with magnetically driven stirring. Small stirring bars were used to agitate the solutions in these cases.

In the case of microwave-heated reactions, all reagents, dispersed or dissolved in water, were charged into a 90-mL Qwave 3000 high-pressure vessel (Questron Corporation, Mercerville, NJ) which, in turn, was placed in a Qwave 3000 microwave oven. The temperature inside the vessel was controlled by a microwave-immune temperature control probe with a temperature control of ±2 K. The mixing of the vessel's content was provided by oscillatory shaking of the vessel.

Experimental syntheses outside the 99% yield regions of NBT and KBT were carried out at 473 K using the conventional hydrothermal method without stirring. In some cases stirring was applied to verify if it plays any role in the synthesis. These experiments were performed in order to validate the calculated stability and yield diagrams (cf. Figures 1−4).

Regardless of the hydrothermal technique applied, the obtained powders were vacuum filtered through 0.22 μm Millipore filter paper (Millipore Corporation, Bedford, MA) and rinsed using an excess of ca. 1000 mL deionized water. Subsequently, they were dried overnight at 338 K.

3. Characterization. The obtained powders were characterized by X-ray diffraction analysis (XRD), field emission scanning microscopy (FESEM), specific surface area and thermogravimetric analysis (TGA). XRD was used to identify solid phases in the obtained powders. The powder diffraction profiles were collected with an automated Siemens D-500 diffractometer (Siemens Analytical X-ray Instrument Inc., Madison, WI) using Ni-filtered Cu Kα radiation at 40 keV and 30 mA. The data were collected by a DACO microprocessor in the 20° to 80° range using a step size of 0.04° 2θ and a count time of 2 s. The chemical identity of the products was determined by comparing the experimental X-ray powder patterns to standards compiled by the Joint Committee on Powder Diffraction and Standards[40] (JCPDS). For this purpose, a commercial program (Jade 3.1) was used. Lattice parameters of selected phase-pure alkaline bismuth titanates mixed with silicon used as internal standard were refined using a least-squares program (Jade 3.1) by fitting over the 2θ range 20−80°. In this case, the step size of 0.02° 2θ and the count time of 25 s were used. Also, sizes of individual crystallites of the NBT and KBT powders were calculated from XRD data by the Jade 3.1 program using the Scherer[41] formula. The instrumental broadening was 0.15°.

The morphology (i.e., assessment of particle shape and qualitative size) of the NBT and KBT particles was examined with a field emission scanning microscope (LEO 982 Gemini SEM, LEO Electron Microscopy, Inc., Thornwood, NY) using an accelerating voltage of 5 keV. Representative samples of the NBT and KBT powders dispersed in ethyl alcohol were placed on aluminum stubs coated with carbon adhesive. After drying, they were covered with a sputtered coat of carbon to prevent charging. The size of the particles was semiquantitatively determined by visual inspection of the FESEM images.

Thermogravimetric analysis (951 TA, DuPont Instruments, New Castle, DE) was performed on the selected NBT and KBT samples to determine their weight loss upon heating in air up to 973 K at a heating rate of 10 deg/min and a flow rate of 50 mL/min. A platinum crucible was used for this work.

Specific surface areas were measured by multipoint BET technique using the Coulter SA 3100 surface area analyzer (Coulter Corporation, Miami, FL) and N_2 gas as the adsorbate. Prior to the measurements, samples were vacuum outgassed for 5 h at 473 K.

Results and Discussion

Experimental validation of calculated stability and yield diagrams in the Na−Bi−Ti and K−Bi−Ti hydro-

(40) McLune, W. F., Ed. *Powder Diffraction File: Inorganic Phases*; JCPDS International Centre for Diffraction Data: Swarthmore, PA, 1989.

(41) Cullity, B. D. *Elements of X-ray Diffraction*; Addison-Wesley: Reading, MA, 1978.

thermal systems is shown in Figures 1−4. Experimental points from the computed region of instability of the NBT and KBT phases are denoted by open circles, pluses, and squares. Solid circles show the formation of phase-pure sodium and potassium bismuth titanates.

1. Na−Bi−Ti−H_2O System. A mixture of unreacted titanium dioxide and bismuth titanate was predicted to form in the regions of thermodynamic instability of sodium bismuth titanate. Analysis of the X-ray patterns of reaction products in the Na−Bi−Ti−H_2O system confirms the theoretical calculations in regions that are slightly narrower than those predicted. In particular, $Bi_4Ti_3O_{12}$ and TiO_2 (both anatase and rutile) form at pH below 10.9 or NaOH concentration below 2.0 m (cf. open circles in Figures 1 and 3). As shown by a solid near-vertical line in Figure 3 (NaOH concentration ∼4 m), thermodynamic calculations predicted a sharp transition from a phase mixture of bismuth titanate and titanium oxide to a single-phase region of NBT with a very small phase overlap at high precursor concentrations. However, an analysis of experimental results revealed a region of coexistence of three phases (i.e., $Bi_4Ti_3O_{12}$, TiO_2, and NBT) for NaOH concentration above ∼2.0 m or pH above 10.9 and below the boundary between $Bi_4Ti_3O_{12}$ and NBT. The experimental points are denoted by squares in this region (cf. Figures 1 and 3). In practice, the coexistence region of the above solids may be a result of kinetic inhibitions caused by a slow transformation from one solid phase to another. In some cases (i.e., at the lower input concentration of bismuth equal to 0.05 m), TiO_2 was not seen in the X-ray patterns. This observation can be explained by the fact that the background was relatively high compared to the intensity of broad peaks in the XRD patterns in this region, thus making it difficult to identify solid phases with good accuracy. This may suggest that the products are not fully crystallized and contain an amorphous phase.

In the region of phase-pure NBT (cf. the shaded regions in Figures 1 and 3), our predictions are fully corroborated by the experimental results. According to the visual analysis of X-ray patterns, a single rhombohedral phase NBT (JCPDS Card No. 36-0153) forms at NaOH concentration above 4 m and at pH above 11.4 at 573 K with and without stirring (cf. solid circles in Figures 1 and 3) within 3 days of reaction.

It was of interest to examine a minimum reaction time and temperature necessary to obtain phase-pure NBT. At 473 K, nonstirred reactions lasting a minimum of 24 h resulted in the formation of phase-pure NBT powders. On the other hand, 8 h were sufficient to obtain pure NBT from the stirred reactions carried out at 453 and 573 K using the conventional− or microwave−hydrothermal technique.

Lattice parameters of the obtained NBT powders were calculated to further confirm their phase purity. Table 3 shows that the obtained values compare well with those reported in the literature. A slight difference in the unit cell parameters of samples prepared by various experimental techniques is expected. The hydrothermally synthesized materials may contain lattice water in addition to surface water, which may influence the lattice parameters. To check the amount of the adsorbed and lattice water, TGA analyses were performed on the same powders for which the lattice parameters were calculated. The weight of the examined NBT powders decreases with temperature up to 623 K. No further weight loss was observed at higher temperatures. The total weight loss can be estimated at 1 wt % which is characteristic for hydrothermally synthesized materials.[23−24,29] A slightly higher weight loss (about 1.3 wt %) was observed for samples obtained from reactions lasting 8 h at lower temperature (i.e., 453 K).

Table 3. Unit Cell Parameters of $K_{0.5}Bi_{0.5}TiO_3$ and $Na_{0.5}Bi_{0.5}TiO_3$

$K_{0.5}Bi_{0.5}TiO_3$		$Na_{0.5}Bi_{0.5}TiO_3$		
a (Å)	*b* (Å)	*a* (Å)	α (deg)	references
3.918	4.013	3.886	89.60	40, 17
3.94	3.94	3.88		2*
3.913(3)	3.993(3)	3.891(2)	89.60(5)	18
3.918	3.996	3.891	89.6	11
3.905(2)	4.097(5)	3.887(2)	89.89(3)	this work
3.917(2)	4.001(5)			this work, after calcination

[a] Smolenski et al.[2] assumed the cubic structure of KBT and NBT.

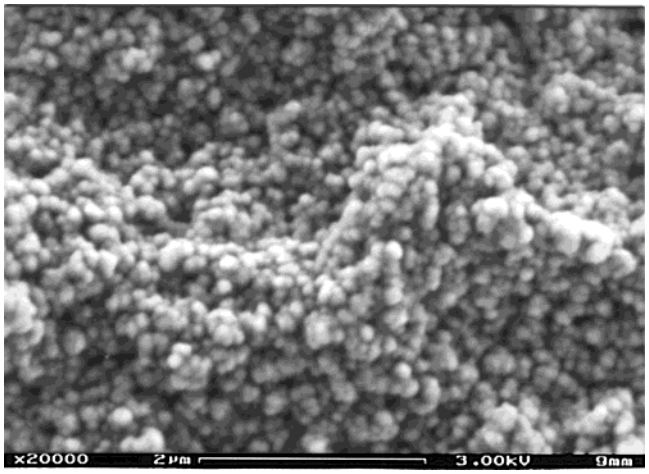

Figure 5. FESEM micrograph of the NBT powders synthesized at the input concentration of $Bi(NO_3)_3 \cdot 5H_2O$, TiO_2, and NaOH equal to 0.1, 0.2, and 12 m, respectively.

Visual analysis of FESEM images shows that NBT powder consists of very small and relatively uniform particles. Spherical crystallites of submicrometer size between 40 and 150 nm can be seen in Figure 5. Crystallite sizes calculated from the XRD peak broadening range from 13 to 28 nm. The measured specific surface areas ranged from 20.0 m^2/g for conventionally obtained NBT powders to 27.6 m^2/g for those obtained using the microwave heating. This corresponds to an estimated average particle size between 50 and 36 nm, respectively. Particles obtained from microwave-heated reactions performed at 453 K and lasting 8 h are smaller (36 nm) than those from oven-heated reactions lasting 3 days at 473 K (50 nm). This difference may be explained by the presence of an amorphous phase, possible agglomeration or even particle growth. On the other hand, the primary particle sizes obtained from the surface area measurements, XRD data and FESEM images differ somewhat from each other. Again, the presence of agglomerates or even a very small content of an amorphous phase may be responsible for the observed difference.

2. K−Bi−Ti−H_2O System. Experiments performed with KOH in the region of KBT instability did not always agree with the predictions of the thermodynamic modeling (cf. Figures 2 and 4). In particular, in some cases it was impossible to identify some of the peaks in the XRD patterns. There are two sources of the above difficulties. First, the peaks were broad and, at the same time, their intensity was relatively low compared with the background, which made assignment to a specific phase difficult. This may also suggest that the obtained powders were not fully crystallized.

Also, it is very likely that we are dealing with an unknown (i.e., not included by JCPDS) phase consisting of potassium, titanium, and/or bismuth and oxygen. A similar problem, which will be reported elsewhere,[36] was encountered in the synthesis of $Bi_4Ti_3O_{12}$ using KOH as a mineralizer. Since our modeling could not take into account a solid phase of unknown stoichiometry, the validation of the stability and yield diagrams outside the stability region of KBT was subject to some limitations.

In general, reaction products from the region of input KOH concentration below 4 m or pH below 11.3 consisted of unreacted TiO_2 (both rutile and anatase), a new solid-phase $Bi_4Ti_3O_{12}$ and an unidentified phase (cf. the crosses in Figures 2 and 4). The intensity of the unidentified peaks in the XRD patterns of the obtained powders declines with an increase in KOH concentration. A mixture of unreacted TiO_2 (anatase), $Bi_4Ti_3O_{12}$, and KBT was identified in the products from reactions performed at pH between 11.3 and 12.2 at 473 K or with the input concentration of KOH between 4 and 7.5 m. This is marked with squares in Figures 2 and 4.

A single tetragonal phase KBT (JCPDS Card No. 36-0339) was obtained in the phase-pure region of the yield diagrams at KOH concentration above 7.5 m and at pH above 12.2 at 573 K with and without stirring (cf. the solid circles in Figures 2 and 4) within 3 days of reaction. The above experimental results validated the theoretical results in the region of phase-pure KBT.

Minimum reaction time and temperature that are necessary for the formation of phase-pure KBT were also investigated. Two days are required to obtain phase-pure KBT at 473 K from the reactions without stirring. However, 8 h were sufficient for the formation of pure KBT powders at the same temperature when stirring was employed. On the other hand, at 453 and 473 K, reactions lasting a minimum of 8 h resulted in the formation of pure KBT using the microwave-hydrothermal technique.

The calculated unit cell parameters for the obtained KBT powders are shown in Table 3. For comparison, lattice parameters are also reported for KBT synthesized using conventional high-temperature solid-state reactions. It can be seen from Table 3 that there is a good agreement between lattice parameters measured by various authors. A slight difference in the unit cell parameters of various samples can be attributed to different experimental techniques for the syntheses. To check the amount of adsorbed and lattice water that may influence unit cell parameters, TGA was performed on the same powders for which the lattice parameters were calculated. The obtained TGA patterns of hydrothermally obtained KBT powders show a weight loss of

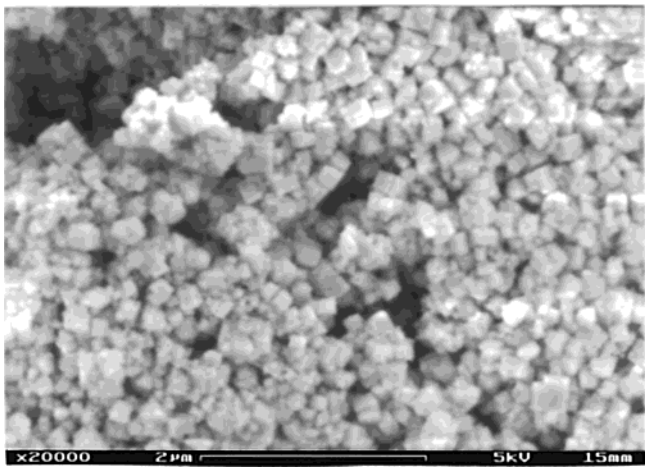

Figure 6. FESEM micrograph of the KBT powders synthesized at the input concentration of $Bi(NO_3)_3 \cdot 5H_2O$, TiO_2, and KOH equal to 0.1, 0.2, and 12 m, respectively.

∼1 wt %. This weight loss takes place up to 623 K and no further weight loss is observed at higher temperatures. A slightly higher weight loss (∼1.5 wt %) was observed for samples obtained from reactions lasting 8 h at the lower temperature (i.e., 453 K). The calculations of lattice parameters were repeated for KBT which was calcined up to 873 K. The observed unit cell parameters (cf. Table 3) for calcined powder are substantially closer to those reported by JCPDS.[40,17]

Visual analysis of FESEM images shows that the KBT powder consists of relatively uniform, submicron particles of cubic shape. Figure 6 shows that their size ranges from ∼25 to 180 nm. Crystallite sizes calculated from the XRD data range from 11 to 34 nm. The measured specific surface areas ranged from 22.6 m^2/g for conventionally obtained KBT powders to 55.7 m^2/g for those obtained using the microwave heating. This results in the average particle size of 45 and 18 nm, respectively. These results are similar to those obtained for the NBT particle size. Therefore, the same reasons for these deviations that were discussed for NBT apply also to KBT.

Conclusions

A thermodynamic model of heterogeneous aqueous electrolyte systems, coupled with experimental results, allowed us to predict the conditions that are appropriate for the hydrothermal synthesis of phase-pure alkaline bismuth titanates. In particular, a synergy between modeling and experiment allowed us to establish standard-state properties of seven solid compounds that exist in the alkali metal−Bi−Ti hydrothermal systems. The predicted conditions are shown in stability and yield diagrams generated for these systems. The model predicts that phase-pure potassium and sodium bismuth titanates can be synthesized hydrothermally from simple precursors at highly alkaline conditions (i.e., pH above 11.4 for NBT and above 12.2 for KBT) at moderate temperatures (above 453 K). The predictions have been experimentally corroborated in the whole alkaline range of the synthesis conditions where NaOH and KOH are used as pH-adjusting agents. The minimum reaction time and temperature were established for the formation of phase-pure KBT and NBT using conventional

and microwave-heated reactions. The particles of the hydrothermal NBT and KBT powders are relatively uniform and of nanometer size.

Acknowledgment. The support of the Office of Naval Research under STTR Contract N00014-97-C-0110 and DARPA is gratefully acknowledged. The authors thank Imre Pozsgai for his assistance in preparing the FESEM micrographs.

CM9906654